frontiers | Frontiers in Marine Science

TYPE Original Research
PUBLISHED 10 November 2022
DOI 10.3389/fmars.2022.1037594

OPEN ACCESS

EDITED BY
Sonja Oberbeckmann,
Leibniz Institute for Baltic Sea Research (LG), Germany

REVIEWED BY
Andy Powell,
Centre for Environment, Fisheries and Aquaculture Science (CEFAS), United Kingdom
Guanpin Yang,
Ocean University of China, China

*CORRESPONDENCE
Tomoo Sawabe
sawabe@fish.hokudai.ac.jp

SPECIALTY SECTION
This article was submitted to Aquatic Microbiology, a section of the journal Frontiers in Marine Science

RECEIVED 06 September 2022
ACCEPTED 19 October 2022
PUBLISHED 10 November 2022

CITATION
Kuroyanagi Y, Tsuchiya J, Jiang C, Mino S, Kasai H, Motooka D, Iida T, Satomi M and Sawabe T (2022) Light response of *Vibrio parahaemolyticus*. *Front. Mar. Sci.* 9:1037594. doi: 10.3389/fmars.2022.1037594

Light response of *Vibrio parahaemolyticus*

Yunato Kuroyanagi[1], Jiro Tsuchiya[1], Chunqi Jiang[1], Sayaka Mino[1], Hisae Kasai[1], Daisuke Motooka[2], Tetsuya Iida[2,3,4], Masataka Satomi[5] and Tomoo Sawabe[1]*

[1]Laboratory of Microbiology, Faculty of Fisheries Sciences, Hokkaido University, Hakodate, Japan, [2]Department of Infection Metagenomics, Genome Information Research Center, Research Institute for Microbial Diseases, Osaka University, Osaka, Japan, [3]Department of Bacterial Infections, Research Institute for Microbial Diseases, Osaka University, Osaka, Japan, [4]Center for Infectious Disease Education and Research (CiDER), Osaka University, Osaka, Japan, [5]Japan Fisheries Research and Education Agency, Fisheries Technology Institute, Shizuoka, Japan

Light is one of the most critical stimuli in the majority of living organisms. In the last two decades, blue light (BL) has become a major subject of attention because of developments in light-emitting diodes (LED). The effects of BL on eukaryotic organisms and phototrophic prokaryotes have been well studied, but the knowledge of its effects on non-phototrophic prokaryotes remains unclear. Since BL can penetrate seawater, it is expected that most prokaryotes living in the ocean possess molecular mechanisms which protect against BL. The aim of this study is to assess the molecular mechanisms of *Vibrio parahaemolyticus* cells against BL as a marine bacterial model compared to other wavelength light exposures. Physiological and transcriptomic analyses of BL-exposed cells compared to other light treated cells revealed the highest ROS fold change, the highest number of differentially expressed genes (DEGs), and up-regulation in the gene responsible to not only compatible solute such as glycine betaine and ectoine but also iron-sulfur biosynthesis related to ROS formation. Furthermore, red light (RL) up-regulated the expression of cryptochrome DASH, a protein known to be excited by BL, and orange light (OL) decreased the expression of thermostable direct hemolysin (TDH), suggesting that OL attenuates the virulence of *V. parahaemolyticus*. In addition, the expression of VtrA (*V. parahaemolyticus* type III secretion system 2 (T3SS2) regulator A) but not VtrB (*V. parahaemolyticus* T3SS2 regulator B) increased under both light treatments, indicating that light exposure is unlikely to be involved in T3SS2-mediated pathogenicity. These results expand our knowledge on unique light responses in non-phototrophic marine prokaryotes.

KEYWORDS

blue light, *vibrio parahaemolyticus*, ROS, RNA-Seq, light response

Introduction

Living organisms respond to various environmental stimuli. Among these stimuli, light is one of the critical stimuli for most living organisms affecting their physiology, behavior, and ecology (Correa et al., 2013; Tardu et al., 2017; Pattison et al., 2018; Sánchez de Miguel et al., 2022). In the last couple of decades, blue light (BL), defined to be 380 nm to 500 nm lights, has become the subject of attention because of developments in light-emitting diodes (LED) and its uses worldwide (Pattison et al., 2018; Sánchez de Miguel et al., 2022). BL has been reported to affect various eukaryotic organisms; e.g. acute melatonine suppression in humans (Pattison et al., 2018), severe retinal degeneration of the eye of rats (Grimm et al., 2001), survival of the pupa *Culex pipiens molestus* (Hori et al., 2015), and induction of photophobic response due to photoactivation of adenylate cyclase in *Euglena gracilis* (Iseki et al., 2002; Ozasa et al., 2017). Responses to BL in phototrophic bacteria have also been well studied; e.g. negative phototaxis by illuminations of 360 nm ultraviolet A ray (UVA), 470 nm BL, and high intensity red light (RL) between 600-700 nm in a *Synechocystis* (Choi et al., 1999; Ng et al., 2003), repression of genes responsible for structural proteins of the photosynthetic complex by BL illumination in *Rhodobacter sphaeroides* under semi-aerobic growth, and identification of the blue light-dependent sensory transduction (Braatsch et al., 2002).

Since BL responses are likely to be present in all domains of life, knowledge of BL effects has been also accumulated in non-phototrophic bacteria (Ávila-Pérez et al., 2006; Tschowri et al., 2009; Tardu et al., 2017; Yoshida et al., 2017 etc.), however, this knowledge lags behind those on eukaryotes and phototrophic prokaryotes. Currently, these are only a few reports on BL effects on non-phototrophic bacteria; identification of various BL-accepting domains such as Light-Oxygen-Voltage (LOV) domain of YtvA protein in *B. subtilis* (Ávila-Pérez et al., 2006) and the BLUF domain of YcgF protein in *E. coli* (Tschowri et al., 2009), and BL triggered reactive oxygen species (ROS) increased photo-oxidative stress in *Porphyromonas gingivalis* (Yoshida et al., 2017) and *V. cholerae* (Tardu et al., 2017) cells. In *B. subtilis*, sigma factor B (σ^B) regulated by the BL stimulus triggered general stress responses (Ávila-Pérez et al., 2006), or suppression of the metalloregulatory (MerR)-like repressor protein YcgE after BL exposure through BLF domain of YcgF protein affected the expression of downstream extracellular polysaccharide and cholanate synthesis genes, which further caused the formation of a thick biofilm (Tschowri et al., 2009). An anti-sigma factor ChrR and a putative MerR were identified as being responsible for BL response regulation in *V. cholerae* (Tardu et al., 2017). In addition, molecular mechanisms of red-light sensing by phytochromes and blue-light sensing by LOV domain proteins have been well studied in plant associated microbes (Beattie et al., 2018). Bacteriophytochromes function to mediate light-regulated suppression of virulence, motility, and conjugation in some phytopathogens and light-regulated induction of the photosynthetic apparatus in a stem-nodulating symbiont (Beattie et al., 2018). Bacterial LOV proteins also influence light-mediated changes in both symbiotic and pathogenic phenotypes (Beattie et al., 2018).

BL can penetrate seawater deep in the ocean, so most prokaryotes, even in non-phototrophic prokaryotes (Duanmu et al., 2017), living in the ocean possess conserved or unique light-accepting proteins and/or molecular mechanisms to protect or respond to BL similar to those retained in terrestrial prokaryotes (Tardu et al., 2017). In fact, different types of BL photoreceptors such as phototropins, cryptochromes (CRYs), and proteins containing BLUF domains and LOV domains to sense the light have been identified in most of marine bacteria (Tardu et al., 2017). However, not only the effects of BL against marine bacteria but also the molecular mechanism in those cells treated with BL have not been fully elucidated yet. *V. parahaemolyticus* is a Gram-staining negative halophilic bacterium that occurs widely in marine and brackish environments, and it is associated with a wide variety of marine animals (Shinoda, 2011; Gomez-Gil et al., 2014; Matsuda et al., 2019a). Portion of strains in this bacterial species show pathogenicity to not only humans but also crustaceans (shrimps and crabs) (Gomez-Gil et al., 2014; Lee et al., 2015; Zhang et al., 2016). *V. parahaemolyticus* and related species live in both shallow and deep-sea environments (Raguénès et al., 1997; Hasan et al., 2015), so unique physiology and survival strategies of this lineage of bacterial species against not only BL but also other light sources are to be expected. Furthermore, genomic and transcriptomic analyses of *V. parahaemolyticus*, in particular, using the strain RIMD 2210633 (serotype: O3:K6), reveals that major genes responsible for the pathogenicity to humans are on the small chromosome, presence of pathogenicity island, called *V. parahaemolyticus* Pathogenicity Island, Vp-PAI, the presence of two sets of genes responsible for type III secretion system (T3SS), and the expression control by environmental stimuli (Makino et al., 2003; Park et al., 2004a; Park et al., 2004b; Ono et al., 2006; Sugiyama et al., 2008; Broberg et al., 2011; Shinoda, 2011; Matsuda et al., 2019a; Matsuda et al., 2019b). T3SS2 is on the Vp-PAI (Matsuda et al., 2019a; Matsuda et al., 2019b). Therefore, in both ecophysiological and evolutionary terms, *V. parahaemolyticus* could be an excellent model marine bacterium to study BL response because of their multiple occurrences in both marine and human associated environments, and accumulated knowledge on their genomes and gene regulations. However, there is little knowledge on how *V. parahaemolyticus* responds to BL, and how BL affects *V. parahaemolyticus* cells, and the gene expression on the pathogenicity (Pazhani et al., 2021). Here, we report the effects of BL on *V. parahaemolyticus* survival and the cellular light responses against BL compared to the effects of the other lights such as UVC, orange light (OL) and red light (RL) as controls

10.3389/fmars.2022.1037594

Materials and methods

Microbial strains and growth conditions

V. parahaemolyticus RIMD 2210633 (serotype O3:K6) was used in this study. The strain was kept at -80°C in 20% glycerol. In each experiment, the glycerol stock was recovered, purified, and used for later experiments. For preculture, the strain was cultured in 100 mL of Tryptic Soy Broth (Becton, Dickinson and Company, New Jersey, USA) supplemented with 2% NaCl (TSB +2% NaCl) using a rotary shaker (FMC-100, EYELA, Tokyo, Japan) at 120 rpm, 37°C, for 16 hours in darkness. The 1 mL of preculture was inoculated into 100 mL TSB+2% NaCl, and then cultured using a rotary shaker at 120 rpm, 37°C, in darkness, until the optical density of cell suspension reached 0.5 at OD620. The culture was transferred to two 50 mL Falcon tubes, and then cells were harvested using centrifugation at 5,000×g for 10 min at 25°C (Avanti HP-26 XP, BECKMAN COLTER, Japan, Tokyo). The pellet was washed twice using Potassium Phosphate Buffer (PPB; 1.4 g K_2HPO_4, 0.6 g KH_2PO_4, 20 g NaCl, 1 mL of 100 mM EDTA up to 1 L distilled water) supplemented with 2% NaCl (PPB+2% NaCl), suspended in 30 mL of PPB+2% NaCl, and then used for the light exposure experiments.

Light exposures

All the following experiments were performed in a dark room. A total of 2 mL of cell suspension was dispensed to disposable polystyrene dishes (40 mm in diameter and 13.5 mm in height), and then exposed to UVC (253.7 nm), BL (minimum wavelength (min.WL): 426 nm, maximum wavelength (max.WL): 525 nm, peak wavelength (peakWL): 456 nm), OL (min.WL: 500 nm, max.WL: 860 nm, peakWL: 620 nm) or RL (min.WL: 584 nm, max.WL: 860 nm, peakWL: 634 nm). For BL, OL, and RL experiments, each light from a fiber light source (FIBER OPTIC LIGHT SOURCE, Nikon, Japan) was selected using a filter (BL, OL: Spectral Line Band-pass Filter, Sigmakoki, Japan, RL: Sharp Cut Filter, Sigmakoki, Japan), photon flux density of each was adjusted to 50 μmoles/m^2/s, and then it was exposed to the cell suspension for 45 minutes. Due to extreme high bactericidal effects of the UVC at the same photon flux density of BL, OL, and RL, the UVC exposure was shortened to 30 seconds using a germicidal lamp (60 μW/cm^2, Germicidal lamp GL-4, Panasonic, Japan). The dark control cells were prepared in the same manner without any light exposures, and used as a negative control to compare physiological states and transcriptomic profiling of the light exposed cells.

To set time for exposure of BL, OL and RL in RNA-Seq experiments, the time to maximize ROS production was selected. For setting the time for the UVC exposure, the time giving a 50% cell survival rate was selected.

Survival rate

Viable bacterial counts were counted using the dilution plate method. Cell suspension was inoculated onto Tryptic Soy Agar supplemented with 2% NaCl (2% NaCl+TSA) (Becton, Dickinson and Company, New Jersey, USA), incubated at 37°C, and then viable bacterial colonies were counted. Viable bacterial counts of the cell suspension exposed to each light versus those left to stand in darkness (control) were measured as the survival rate. Using various light irradiation times from 10 seconds to 60 seconds in UVC, and in BL, OL and RL from 15 minutes to 60 minutes, changes in survival rates were measured.

Measurement of damaged cells

Live/Dead Cell Staining Kit (BioVision, San Francisco, USA) was used for the measurement of the damaged cells after light exposures. SYTO9 in SolutionA can stain all bacterial cells with not only intact cell membranes but also damaged cell membranes, but propidium iodine in SolutionB can only permeate damaged cell membranes and weaken the SYTO9 fluorescence, so bacterial cells with damaged cell membranes were red fluoresced. The *V. parahaemolyticus* cell suspensions after light exposures were centrifuged, washed, and suspended in 2% NaCl+PPB. These cell suspensions were used for the Live/Dead staining according to manufacturer's instruction. A dark control and a dead cell sample suspended in 70% of 2-propanol were prepared to confirm the staining had completed. In brief, 500 μL of cell suspension was dispensed to a sterilized 1.5 mL tube, and then mixed with 1.5 μL of the staining mixture comprised of SolutionA : SolutionB=1:1 at room temperature in the dark for 15 minutes. The stained live and dead cells were observed using a fluorescence microscope (Axiophoto, Zeiss, Oberkochen, Germany) at excitation spectra of 400 nm and 490 nm, and the number of cells in each was enumerated. The ratio of cells with damaged cell membranes was calculated based on total stained cells.

Assessment of photo-oxidative stress

DCF-DA (2',7'-Dichlorofluorescin diacetate, SIGMA-ALDRICH, St. Louis, USA) was used to detect total ROS production. After harvesting and washing the *V. parahaemolyticus* cells, the cells were suspended in 29.97 mL of 2% NaCl+PPB, the 30 μL of 10 mM DCF-DA solution was added and left to stand at 37°C for 30 minutes. A total of 2 mL of stained cell solution was dispensed to disposable dishes and exposed to each light type. The RFU (Relative Fluorescein Units) was measured using a microplate reader (Infinite200, TECAN, Männedorf, Switzerland) at excitation and emission spectra of

485 ± 20 nm and 535 ± 25 nm, respectively. Similarly, the RFU of cells kept in darkness was measured as a control. We made a comparison between the RFU of the control cells and the cells exposed to light, and calculated ROS fold change based on triplicate samples.

Measurement of damaged cells in outer membrane

The ratio of cells damaged in the outer membrane was calculated based on a viable cell percentage obtained from the number of viable bacterial counts on TCBS (Nissui, Tokyo, Japan) compared to that on 2% NaCl+TSA (O'Brien and Colwell, 1985; Alam et al., 2001). The bacterial solutions exposed to each light type and left to stand in darkness as controls were prepared, and then viable bacterial counts were counted on 2% NaCl+TSA and TCBS. The UVC exposure time was set at 30 seconds. The BL, OL, and RL exposure time was set at 45 minutes. The damage to the outer membrane caused by light exposure was then evaluated.

RNA extraction, purification, and RNA-Seq

The 250 μL of cell solution treated with each type of light stress or the dark control were added to 750 μL of TRIzol®LS Reagent (Life Technologies™, New Jersey, USA), mixed well, and then stored at -80°C. Total RNA was isolated from each sample according to the manufacturer's instructions. Isolated total RNA was treated using RQ1 RNase-Free DNase (Promega, Milwaukee, USA) to decompose residual DNA, and then purified using the RNeasy Mini Kit (Qiagen, Maryland, USA). The purity and concentration of total RNA was measured by spectrophotometer (BioSpectrometer, Eppendorf, Hamburg, Germany). Sufficient concentrations of RNA (above 10 μg/μL) were used for RNA-Seq.

RNA-Seq was performed by the Genome Information Research Center, Research Institute for Microbial Diseases, Osaka University (Osaka, Japan). In brief, the composition of total RNA was measured by Agilent2100 Bioanalyzer (Agilent technologies, California, USA). After removal of rRNA from total RNA by using the Ribo-Zero Removal Kit (Bacteria) (Epicentre, California, USA), the amount of RNA above 10 μg/μL was confirmed, and then the library for RNA-Seq was manufactured by using the TruSeq Stranded mRNA Sample Prep Kit (Illumina, California, USA) without poly-A selection. Single read sequences of 75 bp were obtained by HiSeq2500 (Illumina, California, USA).

Bioinformatic analyses

For quality control, mapping, and analysis of the amount of gene expression levels, Genome Traveler (ver. 3.0.48, *In Silico* Biology Inc, Yokohama, Japan) was used. All sequencing reads were filtered at Quality Volume (QV)=25. Filtered reads were mapped on the reference genome sequences, each on both chromosome 1 and 2, of *V. parahaemolyticus* RIMD 2210633 by LAST. After mapping the reads, the RPKM values and mapped read counts on each CDS were outputted. Firstly, RPKM values of dark control and BL exposed cells were compared, and genes showing changes above or below two-fold were identified as Set1B.Genes (Tardu et al., 2017). In the same ways, Set1O.Genes, Set1R.Genes, and Set1U.Genes were identified under OL, RL, and UVC, respectively.

Secondly, for the normalization of mapped gene counts and the statistic test assumed negative binominal distribution, "DESeq" (ver.1.30.0, http://www.bioconductor.org/packages/release/bioc/html/DESeq.html) which is one of the R (ver 3.4.3, https://www.r-project.org/) package was used with the following parameters: p-value and q-value were less than 0.05 to mine Differentially Expressed Gene (DEG) (Anders and Huber, 2010). In each light exposure, DEGs were identified by comparison to the dark control, and then DEGs were set as Set2B.DEGs, Set2O.DEGs, Set2R.DEGs, and Set2U.DEGs, respectively. For further functional analysis, the expression values of Set2B.DEGs under each light type were log2 transformed, and hierarchical clustering was performed on genes using the Euclidian distance with centroid method using the gplots program, which is one of the programs in the R package. After clustering expression values of Set2B.DEGs, a heatmap was generated using the gplots program. The DEGs under each light type were annotated using Rapid Annotation using Subsystem Technology (RAST, version 2.0, rast.nmpdr.org/rast.cgi) (Overbeek et al., 2014), and more detailed protein information was obtained using UniProtKB (http://www.uniprot.org/uniprot/?query=taxonomy:223926). Furthermore, the KEGG (Kyoto Encyclopedia of Genes and Genomes) pathways were identified using DAVID (https://david.ncifcrf.gov/home.jsp) with a p-value<0.05 (Huang et al., 2007). Also, Gene Onthology (GO) terms and enrichment scores were obtained by DAVID with a p-value<0.05, and then network diagrams of GO terms were drawn. As for genes annotated as hypothetical, similar domains and proteins were searched using the HMMER web tool (https://www.ebi.ac.uk/Tools/hmmer/) (Finn et al., 2011). Pfam (http://pfam.xfam.org/) was also used for protein domain search.

Statistical analysis of viable cell counts and ROS measurement data

A Shapiro-Wilk test was performed to test whether data was sampled from the normal population. In the Shapiro-Wilk test, the significance level was tested at 5%, and in the case of p-value<0.05, it was judged that the data did not follow the normal distribution. When the data did not follow normal distribution,

a Wilcoxon rank sum test or Wilcoxon singed-rank test was performed to compare each light stress with the same exposure time or light exposure time in the same color light stress. After that, to compare each light stress, *p*-value was corrected using Tukey's Honestly Significant Difference (Tukey's HSD), and comparison for each light exposure time, FDR was adjusted using the Benjamini-Hochberg method (Benjamini and Hochberg, 1995). When *q*-value<0.05 was satisfied, there was a significant difference. On the other hand, data following the normal distribution was tested for equal variances using the Bartlett test. In the Bartlett test, the significance level was tested at 5%, and in the case of *p*-value<0.05, it was judged that the data was of unequal variance. For unequal variance data, comparison between the two groups was performed in the same way as the method of testing data not following the normal distribution. In the case where the data was of equal variance, after analysis of variance by ANOVA, a paired *t*-test was performed for comparison of each light stress with the same exposure time, and Student's *t*-test was performed for comparison of light exposure time in the same color light stress. After that, to compare each light stress, *p*-value was corrected by Tukey's HSD, and comparison for each light exposure time, FDR was adjusted using the Benjamini-Hochberg method (Benjamini and Hochberg, 1995). When *q*-value<0.05 was satisfied, there was a significant difference.

Results

Survival rate and cell damage by light exposures

In UVC exposure, the survival rate decreased along with exposure times, and the survival rate decreased to below 50% after 30 seconds exposure (Figure 1A). On the contrary, the exposure time did not affect the survival rate ($p > 0.05$) under BL, OL, and RL exposure (Figure 1B).

The ratio of cells with damaged plasma membranes under UVC, BL, OL and RL were 5.0, 3.5, 6.8 and 3.0%, respectively, and little bactericidal effects were observed under these light exposures, nevertheless, the ratio of cells with damaged membranes after 2-propanol treatment reached 76% (Figure 1C).

The ratio of cells with damaged outer membranes was 32.7%, 39.1%, 29.1% and 39.7% under dark, UVC, RL and OL,

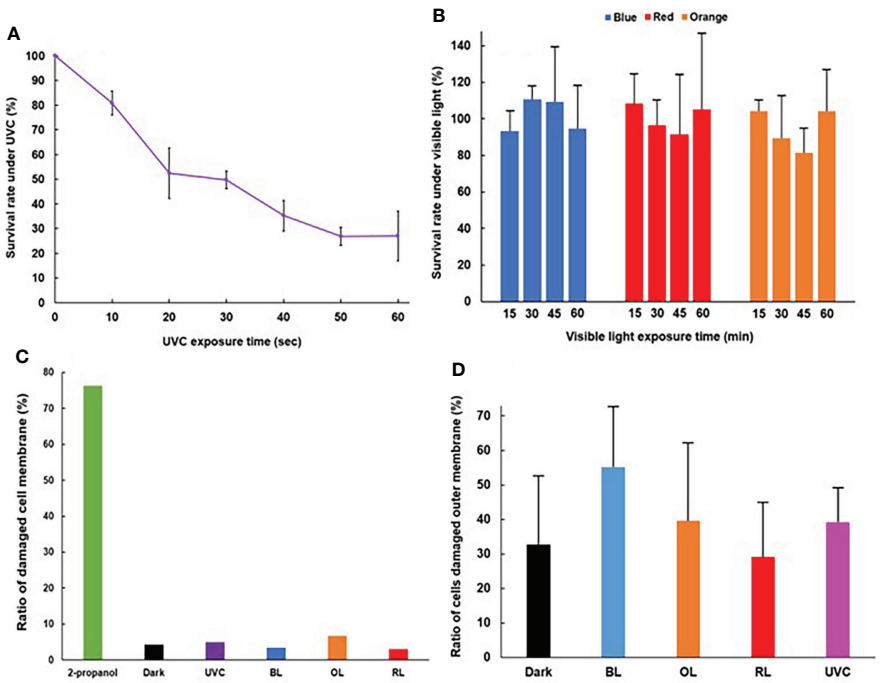

FIGURE 1
Survival rate and cell damages of *Vibrio parahaemolyticus* after exposure of various lights. **(A)** Time course of survival rate after UVC exposure. UVC dose was set at 60 μW/cm^2. (*N* = 3, mean ± standard deviation). **(B)** Time course of survival rate after BL, RL, and OL exposures. Photon flux density was set at 50 μmoles/m^2/s. (*N* = 3, mean ± standard deviation). **(C)** Cell membrane damage. **(D)** Outer membrane damage (*N* = 3, mean ± standard deviation). For **(B, D)**, no statistical significance was detected.

respectively, whereas it increased to 55.2% under BL (Figure 1D). However, there was no significant difference in the ratio in any light treatments (p>0.05).

BL makes *Vibrio parahaemolyticus* form ROS

Under BL exposure, ROS increased along with exposure times, and reached around 100 times that of dark control cells after exposure for 45 minutes (Figure 2A). However, there was no significant difference in the value of ROS fold change of 30-, 45-, and 60-minutes BL exposure (p>0.05). On the other hand, under RL and OL treatments, ROS fold changes did not change significantly over time (Figures 2A, S1). Although ROS tended to increase under UVC exposure, there were no significant differences (Figure 2B).

BL affects the largest number of gene expression

Under each light stress treatment, 899, 835, 638 and 288 genes were identified as Set1B.Genes, Set1O.Genes Set1R.Genes, and Set1U.Genes, respectively (Figure S2). Set2B.DEGs, Set2O.DEGs, Set2R.DEGs and Set2U.DEGs were identified as 77 (up:63, down:14), 59 (up:43, down:16), 76 (up:51, down:25) and 9 (up:0, down:9), respectively (Figure 3). In all light exposure, Set2.DEGs were included in the Set1.Genes. Only three genes were found as common DEGs (VP1941: gene similar to carboxynorspermidine dehydrogenase, VP2757: gene similar to argininosuccinate synthase, VP2758: gene similar to acetylglutamate kinase) with down-regulation under all light exposures (Figure 3). The highest number of genes with variable expression was observed in the BL treatment (Figure 3 and Table S1). All Set2.DEGs were conserved among *V. parahaemolyticus* strains based on genome BLAST searches. Therefore, subsequent functional and pathway analyses on Set2B.DEGs were further performed.

Genes responding to BL are mostly solute- and iron-sulfur cluster-related genes

Unique Set2B.DEGs were counted to be 28 (Figure 3 and Table S1). For further visualization of the changes in gene expression by BL exposure, we performed clustering and heat mapping of Set2B.DEGs (Figure 4). A total of 14 DEGs in Set2B.DEGs were found to have over 30-fold changes, and these 14 DEGs were newly designated as Set3.DEGs (Table S2).

KEGG enrichment analysis of Set2B.DEGs revealed significant upregulation (p<0.05) of three pathways: 1) glycine, serine and threonine metabolism, 2) phenylalanine, tyrosine and tryptophan biosynthesis and valine, and 3) leucine isoleucine degradation (Table S3). All pathways are involved in amino acid metabolism, and genes related to glycine, serine and threonine metabolism were most significantly up-regulated (p<0.05). The only pathway significantly down-regulated (p<0.05) was arginine biosynthesis (Table S3). Two photolyase genes, VPA0204 and VPA1471, were up-regulated (Table S1).

GO term enrichment analysis of Set2B.DEGs revealed 22 significant (p<0.05) GO terms, 19 of which belonged to biological processes, 3 to molecular functions, and none to cellular components. GO terms detected as biological processes were divided into five groups, and the lowest GO terms in each group were 1) glycerol-3-phosphate metabolic processes, 2) protein-chromophore linkage processes, 3) glycine betaine biosynthetic processes from choline, 4) iron-sulfur cluster assembly, and 5) arginine-glutamine family amino acid biosynthetic process. Glycerol-3-phosphate metabolic processes, protein-chromophore linkage, glycine betaine biosynthetic

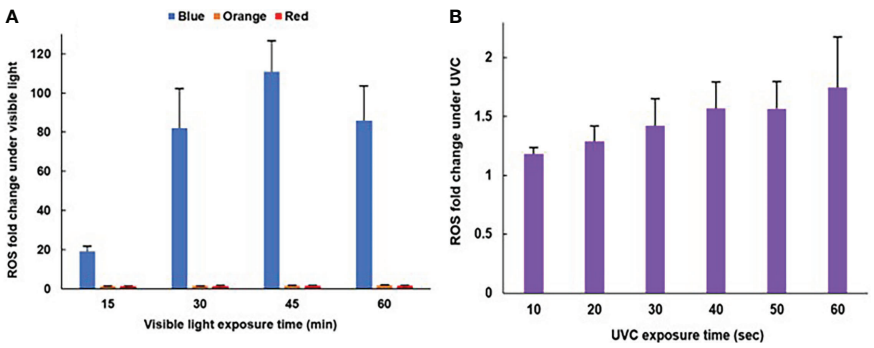

FIGURE 2
Time course of ROS generation after light exposures. **(A)** BL, OL, RL exposures (N=5, mean ± standard deviation) (see Figure S1 for a scale enlarged bar plot for OL and RL). **(B)** UVC exposure (N=5, mean ± standard deviation). For **(B)**, no statistical significance was detected.

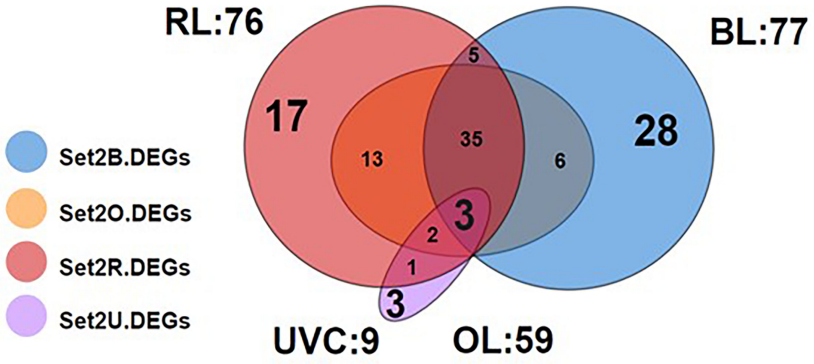

FIGURE 3
Venn diagram of Set2.DEGs. Blue, orange, red and purple color indicate BL, OR, RL and UVC exposure, respectively. A total of 77, 59, 76, and 9 genes were identified as Set2B, Set2O, Set2R, and Set2U.DEGs, respectively. The largest number of BL unique DEGs was observed.

processes from choline, and iron-sulfur cluster assembly were significantly (p<0.05) up-regulated. The group of GO terms significantly (p<0.05) down-regulated was the Arginine-Glutamine family amino acid biosynthetic process (Figure 5A). Of the five groups of GO terms, the glycine betaine biosynthetic process from choline was the most abundant in Set2B.DEGs. Glycine betaine is known to be a compatible solute for *V. parahaemolyticus*. Ectoin synthesis gene (*ectA*), another known compatible solute, was also upregulated. On the other hand, GO terms detected as molecular functions were divided into two; 1) 2 iron, 2 sulfur cluster binding and 2) tryptophan synthase activity (Figure 5B). Both GO terms were assigned to up-regulated DEGs.

With the exception of VP1119, VP1120, and VP1123, Set3B.DEGs were identified to be hypothetical proteins (Table S2). But further domain searches predicted that VP1121 and VP1125 had significantly (E-value <0.01) similar domain proteins (Table S4). VP1121 were suggested to have functional

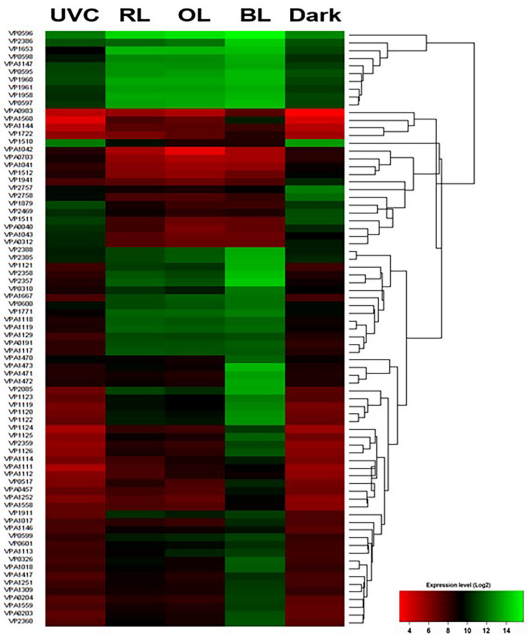

FIGURE 4
Heatmap of Set2B.DEGs. See Table S1 for gene product function. Expression levels are represented by color: green, higher expression level; red, lower expression level based on Log2 fold change.

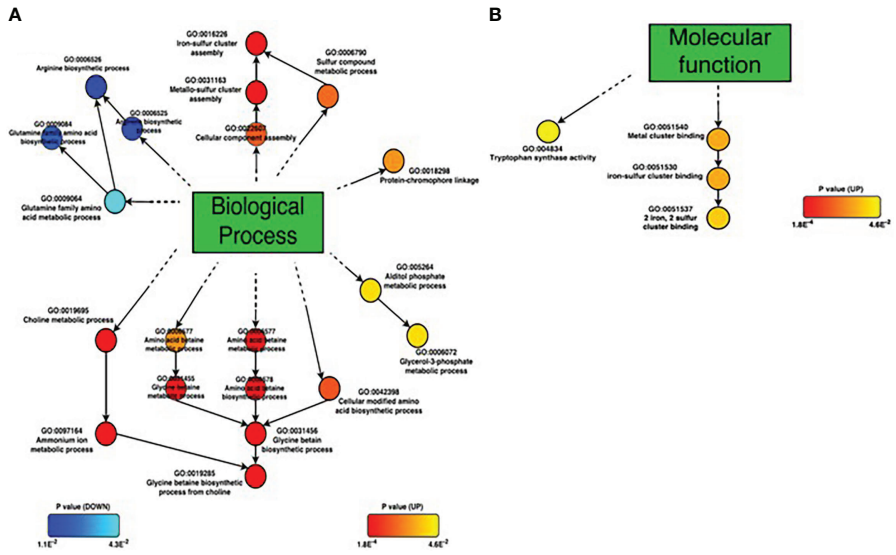

FIGURE 5
GO term enrichment analyses ofSet2B.DEGs. **(A)** Biological process, **(B)** Molecular function. Circles represent each GO term; up-regulated GO terms are shown by red to yellow, and down-regulated GO terms are shown by blue to cyan. GO terms closed to red and blue colors are significantly regulated based on *p*-value.

domains related to cofactors and coenzymes such as flavin and NAD(P). On the other hand, VP1125 was found to have domains similar to chalcone isomerase-like proteins, but chalcone biosynthesis pathways have never been found in prokaryotes.

RL and UVC-specific responsive genes

In Set2DEGs, 17 DEGs responded in an RL-specific manner (Figure 3 and Table S1). For RL-specific DEGs, GO term enrichment analysis was performed and a network diagram was drawn (Figure S3). The GO terms for biological processes were obtained, and there were no significant up-regulated terms among them ($p>0.05$). Down-regulated terms yielded a group of GO terms for arginine-glutamate family metabolism ($p<0.05$) (Figures S4, S5). DEGs responded to UVC were *trpE* (VP1956) and *trpG* (VP1957) related to tryptophane biosynthesis, and oligopeptide ABC transporter (VP2088) (Table S1 and Figure S6). All three were downregulated.

There were genes on Vp-PAI that commonly responded to light stress

No genes on Vp-PAI were included in Set2.DEGs, but 6, 2, 6 and 1 Set1.Genes on Vp-PAI after BL, RL, OL and UVC exposures, respectively, were found (Table S5). The expression of VPA1332 (*vtrA*) tended to increase under all light stresses. VPA1314 (thermostable direct hemolysin A) and VPA1378 (thermostable direct hemolysin S) were likely to be down-regulated by OL exposures.

Discussion

There is growing interest in the light response of all domains of life in the perspective of evolutionary conservation of physiological effects (Correa et al., 2013; Tardu et al., 2017; Pattison et al., 2018; Sánchez de Miguel et al., 2022). Since BL can penetrate deep in the ocean, it is assumed that there are non-photosynthetic marine bacteria that maintain unique BL responses (Duanmu et al., 2017; Tardu et al., 2017). In fact, the BL response has been examined in *V. cholerae* and the ROS triggered photooxidative stress response though an anti-sigma factor, ChrR, and a putative metalloregulatory-like protein, MerR, was proposed (Tardu et al., 2017). Three genes (VC1392, VC1814, and VCA0057) encoding cryptochrome/photolyase family (CPF) members were up-regulated, but uses of knockdown mutants did not identify these genes to be involved in BL-mediated responses (Tardu et al., 2017). No genes responsible to pathogenicity and virulence of *V. cholerae* were DEGs responding to BL (Tardu et al., 2017). *V. parahaemolyticus* may have various adaptive capacities because of the diversity of its habitat and pathogenicity, but knowledge of the response of *V. parahaemolyticus* to not only BL but also the other types of lights is limited (Pazhani et al., 2021). In this study, our aim is to elucidate light responses of *V.*

parahaemolyticus based on physiological and transcriptome experiments. Not surprisingly, BL exposure regulates gene expression through ROS in *V. parahaemolyticus*, similar to *V. cholerae*, which possesses photolyase/cryptochrome (CPF) member proteins as the sole BL photoreceptors (Tardu et al., 2017). In addition, BL also up-regulated the gene responsible for not only CPF members but also compatible solute such as glycine betaine and ectoine, and iron-sulfur biosynthesis related to ROS formation in *V. parahaemolyticus*. Interestingly, OL was likely to repress the TDH expression, suggesting that OL may attenuate the virulence of *V. parahaemolyticus*. In addition, the expression of VtrA but not VtrB increased under RL and OL treatments, indicating that light stress is unlikely to be involved in T3SS2-mediated pathogenicity. Each light stress response is further discussed below.

Physiological effects of each light on *Vibrio parahaemolyticus*

UVC induces a significant decrease in survival rates of *V. parahaemolyticus* without ROS accumulation. On the contrary, BL did not cause decreases in cell viability and survival but significant increases in ROS accumulation in this bacterium. As in *V. cholerae*, BL triggers ROS production in *V. parahaemolyticus*. In *V. cholerae*, extracellular ROS is formed by the reaction of Na^+-NQR (Na^+-driven NADH-quinone oxidoreductase) on the cell membrane (Lin et al., 2007), so it is possible that in *V. parahaemolyticus*, ROS production by BL exposure may be similar to that in *V. cholerae*. OL or RL irradiations were unlikely to affect not only cell viability but also the ratio of dead bacteria, neither in ROS accumulation.

Gene expression by BL exposure

Compatible solutes, iron-sulfur cluster biosynthesis genes, ROS responsive genes, and light recovery enzyme genes were significantly up-regulated by BL treatment, each feature is discussed below.

Solute biosynthesis genes are upregulated by BL treatment

GO term enrichment analysis of Set2B.DEGs showed that the glycine betaine biosynthesis pathway from choline (*betABI*; VPA1112, VPA1113, VPA1114) and its transporter, the ABC transporter gene VPA1111, as well as the ectoin synthesis gene (*ectA*; VP1722) were significantly up-regulated. KEGG enrichment analysis showed a significant increase in the glycine biosynthesis pathway, indicating that BL exposure up-regulates metabolic pathways related to glycine betaine. VPA1111, VPA1112, VPA1113, and VPA1114 were also found in the Set2O.DEGs. Glycine betaine, also called trimethylglycine, and ectoin are synthesized as compatible solutes in *V. parahaemolyticus* and are involved in osmotic adaptation (Ongagna-Yhombi and Boyd, 2013), but ectoin is the only compatible solute in *V. cholerae*, and that is from aspartic acid (Pflughoeft et al., 2003). In *V. parahaemolyticus*, these solutes are synthesized in a growth phase-dependent manner under high salinity (6% NaCl) conditions (Ongagna-Yhombi and Boyd, 2013), and *betABI* expression has also been reported to increase with temperature stress (Ma et al., 2017). As discussed later, the up-regulation of *betABI* was observed after OL exposure as well, that might be caused by temperature stress. As OL is more easily absorbed by water than BL, which may cause a temperature change in cellular fluid fraction, so significant up-regulations of solute-related genes by BL might be triggered to metabolize precursors of each osmolyte. The BL induced osmolyte gene expressions need to be elucidated in the future.

Expression of iron-sulfur cluster biosynthesis genes is also increased by BL treatment

GO term enrichment analysis of Set2B.DEGs revealed a significant increase in the expression of iron-sulfur cluster biosynthesis genes: *iscU* (VP0597), *iscA* (VP0598), *hscB* (VP0599), *hscA* (VP0600) and ferredoxin (VP0601). Iron-sulfur clusters are coordinately bound within proteins in the form of 2Fe-2S and 4Fe-4S and are involved in chemical reactions as Rieske centers (Conte and Zara, 2011). Iron-sulfur clusters are present in all organisms and are involved in many vital cellular processes such as respiratory chain, central metabolism, gene expression regulation, RNA modification, and DNA repair and replication (Py and Barras, 2010). When iron-sulfur clusters are destabilized by ROS, their structure changes and iron ions are released, and further ROS are formed by Fenton reactions between hydrogen peroxide, one of the ROS, and free iron ions (Remes et al., 2015). There are three iron-sulfur cluster synthesis systems in bacteria, ISC, SUF, and NIF (Py and Barras, 2010; Remes et al., 2015), and based on annotation results, ISC and NIF-related genes were present in *V. parahaemolyticus*. In this study, BL exposure increased the expression of a series of iron-sulfur cluster synthesis systems (ISC machinery; *iscRSUA*, *hscA/B* and Ferredoxin), which are controlled by the transcriptional regulator *iscR*. This is presumably explained that the ROS produced by BL exposure deprived the iron-sulfur clusters in the iron-sulfur protein of iron ions, and ISC was activated to compensate for this

deprivation. In addition, since free iron generates ROS, the increased expression of ISC in *V. parahaemolyticus* may indicate the generation of new ROS.

Genes responsive to ROS

In *V. cholerae*, ROS is formed by Na^+-NQR and coenzyme Q, causing transcriptional regulation through the transcriptional regulators ChrR and MerR-like regulators; ChrR is an anti-sigma factor that represses σE (Tardu et al., 2017); MerR-like regulators are transcriptional activators which respond to oxidative transcriptional activators that respond to stimuli such as stress, heavy metals, and antibiotics (Brown et al., 2003). Therefore, we investigated whether Set2B.DEGs contain genes encoding similar proteins or not, and found a ChrR (VP2357) and a MerR-like regulator (VPA1472) genes, whose expression levels were 28.8- and 41.1-fold higher than those of dark control, respectively. Thus, it was suggested that gene expression is regulated by ROS in *V. parahaemolyticus* similar to that in *V. cholerae*. It was also suggested that LitR, a MerR-like regulator in *Streptomyces griseus*, may not only be involved in transcriptional regulation but also act as a photoreceptor sensor (Takano et al., 2006). However, no photoreceptor PAS (Per Arnt Sim) domains in MerR-like regulators similar to those in *Streptomyces griseus* were found in *V. parahaemolyticus*. Thus, the MerR-like regulator of *V. parahaemolyticus* is not involved in photoreception. Glutathione peroxidase was also among the BL-specific DEGs (Table S1). Glutathione peroxidase is an enzyme that primarily converts glutathione oxidized by ROS back to its reduced form (Miyamoto et al., 2003), confirming that BL can activate ROS removing mechanisms in *V. parahaemolyticus*.

BL irradiation increased expression of the cryptochrome/photolyase family

V. parahaemolyticus possess VPA0203 (cryptochrome DASH), VPA0204 (putative photolyase) and VPA1471 (CPD photolyase; Cyclobutane Pyrimidine Dimer photolyase) as known BL response protein genes (Su et al., 2015). These three proteins belong to the cryptochrome/photolyase family (CPF), which are light-recovery enzymes known to be stimulated by BL, and directly repair CPD, DNA dimerization damages. Cryptochrome DASH mainly repairs CPD on single-stranded DNA, while CPD photolyase repairs CPD on double-stranded DNA (Kavakli et al., 2017). In this experiment, all CPFs of *V. parahaemolyticus* were found in Set2B.DEGs, confirming that BL exposure enhances direct DNA repair capacity. These genes similar to CPF members were candidates for BL-receptor proteins, but these genes were similar to genes up-regulated under BL exposure in *V. cholerae*, not being involve in BL-mediated gene expression (Tardu et al., 2017).

Set3DEGs as BL exposure responses

Based on the clustering of expression values for Set2B.DEGs, Set3.DEGs included gene sets VP1119, VP1120, VP1122, VP1123, VP1124, VP1125, and VP1126, which are thought to be co-expressed. VP1123 is a gene encoding a putative cyclopropane fatty acid phospholipid synthase (CFA synthase); CFA is a component of bacterial cell membrane lipids, and CFA synthase forms cyclopropane rings on unsaturated fatty acids in membrane phospholipids using S-adenosylmethionine as a methyl donor (Zhang and Rock, 2008), and CFAs have been reported to protect cells from various injuries. In *E. coli*, it has been reported that CFAs are formed by heat and pressure stress treatment (Chen and Gänzle, 2016). It has also been reported that under oxidative stress, CFA decreases the proton permeability and efflux capacity of the plasma membrane and maintains intracellular pH homeostasis (Shabala and Ross, 2008). Furthermore, increased CFA synthase gene expression has been observed in *V. cholerae* upon BL irradiation, which is thought to protect cells from ROS and minimize their susceptibility to further oxidative damage (Tardu et al., 2017). Therefore, the reason for the lack of an increase in plasma membrane-damaged dead cells may be that CFA synthases prevent oxidative damage to membrane lipids by ROS by modifying plasma membrane phospholipids. Furthermore, Set2B.DEGs contained a *blc*-like gene (VPA1018) encoding the lipoprotein Blc, but not Set3DEGs, and its expression level was 11.4-fold higher in the dark control cells upon BL irradiation. It has been suggested that BL damages the outer membrane *via* ROS, and the expression of *blc* increased in response (Campanacci et al., 2006). The above suggests that the reason for the increases in numbers of outer membrane-damaged cell but not in those of plasma membrane-damaged dead cells under BL exposure may be a protection of the plasma membrane by addition of cyclopropane rings by CFA activity.

Genes expression by RL and OL exposures

GO term enrichment analysis of RL-specific responsive DEGs revealed that the arginine biosynthetic pathways (VP2653, VP2756, and VP2759) were reduced. GO term enrichment analysis of Set2B.DEGs also showed a decrease in the arginine-glutamate family biosynthetic pathway. DEGs also contained arginine biosynthesis genes, which were also reduced in both Set2O.DEGs and Set2U.DEGs. These results indicate that this amino acid biosynthesis pathway is suppressed in general light stress. Broad Set2DEGs comparison revealed that arginine metabolism-related genes were well repressed by RL and OL (Figure S3). KEGG pathway mapping further identified N-acetylglutamate semialdehyde is synthesized from glutamate (VP2371, VP2756, VP2758, VP2759) and arginine from ornithine (VP2653, VP2756,

VP2757) were well suppressed under RL exposure (Figure S4). Those pathways were also suppressed to almost the same extent under OL exposure. Thus, it was suggested that the arginine biosynthetic pathway of *V. parahaemolyticus* is completely suppressed by RL and OL exposures. In addition, the glutamate biosynthesis gene, which is required for arginine biosynthesis, was not included in all Set2.DEGs, and only the arginine biosynthesis gene was significantly suppressed ($p<0.05$). Thus, the reason for the suppression of arginine biosynthesis may be that glutamate was required for the biosynthesis of another metabolite. Glutamate is involved in a variety of metabolisms, including amino acid metabolism such as histidine and purine, nitrogen metabolism, glutathione metabolism, porphyrin metabolism, and butyrate metabolism. Glutamate may be used for the synthesis of glutathione, an antioxidant known as an antioxidant protection mechanism against ROS (Reynolds and Hastings, 1995), but it is not known whether RL and OL exposures resulted in much lower ROS accumulation than BL, and this could not be the reason why RL and OL most inhibited arginine biosynthesis. In addition, since glutamate is one of the compatible solutes of *V. parahaemolyticus* (Ongagna-Yhombi and Boyd, 2013), it is possible that glutamate is accumulated intracellularly to counteract light stress.

In addition, OL exposure reduced the expression of *tdh1* (VPA1378) and *tdh2* (VPA1314) to less than half that in dark control. Tdh is related to Kanagawa phenomenon (Sakazaki et al., 1968; Nishibuchi and Kaper, 1995; Shinoda, 2011). These genes were found only in Set1O.DEGs, suggesting that OL may not strengthen the virulence of *V. parahaemolyticus*.

Genes expression by UVC exposure

Genes that responded in a UVC-specific manner were *trpE*, *trpG* and oligopeptide ABC transporters involved in tryptophan biosynthesis, all of which were downregulated. The heatmap of the regulation of *trpL*, *trpE*, *trpG*, *trpC*, *trpB1*, and *trpA* genes on the tryptophan operon (*trp* operon) under light irradiation showed that their expression tended to increase under BL, OL, and RL irradiation, while their expression decreased under UVC irradiation (Figure S5). The *trp* operon is a set of genes whose transcription is repressed when tryptophan is abundant and activated when tryptophan is deficient. The reason for this may be that the initial response to UVC irradiation is rapid biosynthesis of tryptophan, but once the concentration reaches a certain level in the cell, it may shift toward repression of transcription of the *trp* operon. In addition, tryptophan, an aromatic amino acid, has been reported to absorb UVC and UVB at 260-305 nm (Holiday, 1936). Furthermore, it has been shown that when tryptophan-containing DNA solutions are exposed to UVCs, tryptophan preferentially absorbs UVCs and reduces DNA damage (Oladepo and Loppnow, 2010). Therefore, it is possible that tryptophan is synthesized to protect DNA from UVC-induced DNA damage, and intracellular tryptophan concentration and localization should be measured before and after UVC irradiation.

UVC is also known to decrease viability and cause dimerization damage to DNA, which is thought to activate DNA repair mechanisms, but DNA repair-related genes were not found in Set2U.DEGs. This could be because the UV intensity was too intense or because the 30-second irradiation did not stress all the bacterial cells.

Pathogenicity and light stress

VPA1332 was upregulated under all light stresses. The VPA1322 product is named to be VtrA, a membrane-bound transcriptional regulator that plays a central role in the expression of the Vp-PAI gene, and VtrA also activates T3SS2 synthesis indirectly by activating transcription of *vtrB* (VPA1348) (Li et al., 2016). BL exposure up-regulated the most in *vtrA*. Upregulation of only *vtrA* gene, but not *vtrB* gene, by light exposures suggests that light stress does not induce T3SS2-mediated pathogenicity. Furthermore, it has been reported that VtrA oligomerizes between DNA-binding domains on the cytosolic sol side when cells are stimulated, activating transcription of *vtrB* (Okada et al., 2017; Matsuda et al., 2019a). It has also been reported that VtrA activates transcription of *vtrB* by forming a complex with VtrC (VPA1333) (Li et al., 2016; Matsuda et al., 2019a), however, we did not find that *vtrC* was included in Set1.Genes.

Conclusion

Light response is ecophysiologically important and conserved in evolutionary terms in all domains of life, but that of non-photosynthetic bacteria has been not fully studied yet. Recent developments of LED devices encourage us to focus on how BL responses effect organisms. In particular, the ocean is a unique medium for selecting various kinds of lights, BL can penetrate seawater deeply, so life in the ocean may foster better biological materials to answer the questions of how marine organisms respond to BL. In this study, using *V. parahaemolyticus* RIMD 2210633, a pandemic strain, as a non-phototrophic marine bacterium model, BL response is accessed using physiological and transcriptomic approaches. Interestingly, *V. parahaemolyticus* responds to BL more than the other light type, and in particular, up-regulation in the gene responsible to not only compatible solute but also iron-sulfur biosynthesis related to ROS formation, but there were no regulations on genes on the pathogenicity. Nevertheless, the population structure of *V. parahaemolyticus* strains was rather complex but clonal in pandemic strains (Chowdhury et al., 2000; Gonzalez-Escalona et al., 2008; Urmersbach et al., 2014), however, genes responding to not only

BL exposure but also to the other lights wavelength are likely to be conserved among *V. parahaemolyticus* strains. These results provide new ecophysiological and evolutionary insights in light responses in non-phototrophic marine bacteria.

Data availability statement

The datasets presented in this study can be found in online repositories. The names of the repository/repositories and accession number(s) can be found below: https://www.ddbj.nig.ac.jp/, DRA014596.

Author contributions

YK, SM, TI, DM, TS conceived, designed and performed the experiments, analyzed the data, visualized the data, and drafted and reviewed the manuscript. JT, HK and MS re-analyzed the data and reviewed the manuscript. All authors contributed to the article and approved the submitted version.

Funding

This study was conducted under the research project for "Improving Food Safety and Animal Health (JPJ002032, 13406381)" funded by the Ministry of Agriculture, Forestry and Fisheries of Japan.

Conflict of interest

The authors declare that the research was conducted in the absence of any commercial or financial relationships that could be construed as a potential conflict of interest.

Publisher's note

All claims expressed in this article are solely those of the authors and do not necessarily represent those of their affiliated organizations, or those of the publisher, the editors and the reviewers. Any product that may be evaluated in this article, or claim that may be made by its manufacturer, is not guaranteed or endorsed by the publisher.

Supplementary material

The Supplementary Material for this article can be found online at: https://www.frontiersin.org/articles/10.3389/fmars.2022.1037594/full#supplementary-material

References

Aívila-Peírez, M., Hellingwerf, K. J., and Kort, R. (2006). Blue light activates the σ b-dependent stress response of *Bacillus subtilis via* YtvA. *J. Bacteriol.* 188, 6411–6414. doi: 10.1128/JB.00716-06

Alam, M. J., Tomochika, K., Miyoshi, S., and Shinoda, S. (2001). Analysis of seawaters for the recovery of culturable *Vibrio parahaemolyticus* and some other vibrios. *Microbiol. Immunol.* 45, 393–397. doi: 10.1111/j.1348-0421.2001.tb02636.x

Anders, S., and Huber, W. (2010). Differential expression analysis for sequence count data. *Genome Biol.* 11, R106. doi: 10.1186/gb-2010-11-10-r106

Beattie, G. A., Hatfield, B. M., Dong, H., and McGrane, R. S. (2018). Seeing the light: the roles of red- and blue-light sensing in plant microbes. *Annu. Rev. Phytopathol.* 56, 41–66. doi: 10.1146/annurev-phyto-080417-045931

Benjamini, Y., and Hochberg, Y. (1995). Controlling the false discovery rate: A practical and powerful approach to multiple testing. *J. R. Statist. Soc. ser.B*, 57, 289–300. doi: 10.1111/j.2517-6161.1995.tb02031.x

Braatsch, S., Gomelsky, M., Kuphal, S., and Klug, G. (2002). A single flavoprotein, AppA, integrates both redox and light signals in *Rhodobacter sphaeroides*. mol. *Microbiol.* 45, 827–836. doi: 10.1046/j.1365-2958.2002.03058.x

Broberg, C. A., Calder, T. J., and Orth, K. (2011). *Vibrio parahaemolyticus* cell biology and pathogenicity determinants. *Microbes Infect.* 13, 992–1001. doi: 10.1016/j.micinf.2011.06.013

Brown, N. L., Stoyanov, J. V., Kidd, S. P., and Hobman, J. L. (2003). The MerR family of transcriptional regulators. *FEMS Microbiol. Rev.* 27, 145–163. doi: 10.1016/S0168-6445(03)00051-2

Campanacci, V., Bishop, R. E., Blangy, S., Tegoni, M., and Cambillau, C. (2006). The membrane bound bacterial lipocalin Blc is a functional dimer with binding preference for lysophospholipids. *FEBS Lett.* 580, 4877–4883. doi: 10.1016/j.febslet.2006.07.086

Chen, Y. Y., and Gänzle, M. G. (2016). Influence of cyclopropane fatty acids on heat, high pressure, acid and oxidative resistance in *Escherichia coli*. int. *J. Food Microbiol.* 222, 16–22. doi: 10.1016/j.ijfoodmicro.2016.01.017

Choi, J.-S., Chung, Y.-H., Moon, Y.-J., Kim, C., Watanabe, M, Song, P. S., et al. (1999). Photomovement of the gliding cyanobacterium *Synechocystis* sp. PCC 6803. *Photochem. Photobiol.* 70, 95. doi: 10.1562/0031-8655(1999)070<0095:POTGCS>2.3.CO;2

Chowdhury, N. R., Chakraborty, S., Ramamurthy, T., Nishibuchi, M., Yamasaki, S., Takeda, Y., et al. (2000). Molecular evidence of clonal *Vibrio parahaemolyticus* pandemic strains. *Emerg. Infect. Dis.* 6, 631–636. doi: 10.3201/eid0606.000612

Conte, L., and Zara, V. (2011). The rieske iron-sulfur protein: Import and assembly into the cytochrome *bc1* complex of yeast mitochondria. *Bioinorg. Chem. Appl.* 2011, 363941. doi: 10.1155/2011/363941

Correa, F., Ko, W.-H., Ocasio, V., Bogomolni, R. A., and Gardner, K. H. (2013). Blue light regulated two-component systems: Enzymatic and functional analyses of light-Oxygen-Voltage (LOV)-histidine kinases and downstream response regulators. *Biochemistry* 52, 4656–4666. doi: 10.1021/bi400617y

Duanmu, D., Rockwell, N. C., and Lagarias, J. C. (2017). Algal light sensing and photoacclimation in aquatic environments. *Plant Cell Environ.* 40, 2558–2570. doi: 10.1111/pce.12943

Finn, R. D., Clements, J., and Eddy, S. R. (2011). HMMER web server: Interactive sequence similarity searching. *Nucleic Acids Res.* 39, W29–W37. doi: 10.1093/nar/gkr367

Gomez-Gil, B., Thompson, C. C., Matsumura, Y., Sawabe, T., Iida, T., Christen, R., et al. (2014). "The family vibrionaceae," in *The prokaryotes – gammaproteobacteria*. Ed. E. Rosenberg, et al (New York: Springer). doi: 10.1007/978-3-642-38922-1_225

Gonzalez-Escalona, N., Martinez-Urtaza, J., Romero, J., Espejo, R. T., Jaykus, L.-A., and DePaola, A. (2008). Determination of molecular phylogenetics of *Vibrio parahaemolyticus* strains by multilocus sequence typing. *J. Bacteriol.* 190, 2831–2840. doi: 10.1128/JB.01808-07

Grimm, C., Wenzel, A., Williams, T., Rol, P. O., Hafezi, F., and Remé, C. E. (2001). Rhodopsin-mediated blue-light damage to the rat retina: Effect of photoreversal of bleaching. *Invest. Ophthalmol. Vis. Sci.* 42, 497–505.

Hasan, N. A., Grim, C. J., Lipp, E. K., Rivera, I. N.G., Chun, J., Haley, B. J., et al. (2015). Deep-sea hydrothermal vent bacteria related to human pathogenic *Vibrio* species. *Proc. Natl. Acad. Sci.* 112, E2813–E2819. doi: 10.1073/pnas.1503928112

Holiday, E. R. (1936). Spectrophotometry of proteins. *Biochem. J.* 30, 795–1803. doi: 10.1042/bj0301795

Hori, M., Shibuya, K., Sato, M., and Saito, Y. (2015). Lethal effects of short-wavelength visible light on insects. *Sci. Rep.* 4, 7383. doi: 10.1038/srep07383

Huang, D. W., Sherman, B. T., Tan, Q., Kir, J., Liu, D., Bryant, D., et al. (2007). DAVID bioinformatics resources: Expanded annotation database and novel algorithms to better extract biology from large gene lists. *Nucleic Acids Res.* 35, W169–W175. doi: 10.1093/nar/gkm415

Iseki, M., Matsunaga, S., Murakami, A., Ohno, K., Shiga, K., Yoshida, K., et al. (2002). A blue-light-activated adenylyl cyclase mediates photoavoidance in *Euglena gracilis*. *Nature* 415, 1047–1051. doi: 10.1038/4151047a

Kavakli, I. H., Baris, I., Tardu, M., Gül, S., Öner, H., Çal, S., et al. (2017). The photolyase/cryptochrome family of proteins as DNA repair enzymes and transcriptional repressors. *Photochem. Photobiol.* 93, 93–103. doi: 10.1111/php.12669

Lee, C.-T., Chen, I.-T., Yang, Y.-T., Ko, T.-P., Huang, Y.-T., Huang, J.-Y., et al. (2015). The opportunistic marine pathogen *Vibrio parahaemolyticus* becomes virulent by acquiring a plasmid that expresses a deadly toxin. *Proc. Natl. Acad. Sci. U.S.A.* 112, 10798–10803. doi: 10.1073/pnas.1503129112

Lin, P.-C., Türk, K., Haüse, C. C., Fritz, G., and Steuber, J. (2007). Quinone reduction by the na^+-translocating NADH dehydrogenase promotes extracellular superoxide production in *Vibrio cholerae*. *J. Bacteriol.* 189, 3902–3908. doi: 10.1128/JB.01651-06

Li, P., Rivera-Cancel, G., Kinch, L. N., Salomon, D., Tomchick, D. R., Grishin, N. V., et al. (2016). Bile salt receptor complex activates a pathogenic type III secretion system. *Elife* 5, e15718. doi: 10.7554/eLife.15718

Makino, K., Oshima, K., Kurokawa, K., Yokoyama, K., Uda, T., Tagomori, K., et al. (2003). Genome sequence of *Vibrio parahaemolyticus*: A pathogenic mechanism distinct from that of *V cholerae*. *Lancet* 361, 743–749. doi: 10.1016/S0140-6736(03)12659-1

Matsuda, S., Hiyoshi, H., Tandhavanant, S., and Kodama, T. (2019a). Advances on *Vibrio parahaemolyticus* research in the postgenomic era. *Microbiol. Immun.* 64, 167–181. doi: 10.1111/1348-0421.12767

Matsuda, S., Okada, R., Tandhavanant, S., Hiyoshi, H., Gotoh, K., Iida, T., et al. (2019b). Export of a *Vibrio parahaemolyticus* toxin by the sec and type III secretion machineries in tandem. *Nat. Mirobiol.* 4, 781–788. doi: 10.1038/s41564-019-0368-y

Ma, Y., Wang, Q., Gao, X., and Zhang, Y. (2017). Biosynthesis and uptake of glycine betaine as cold-stress response to low temperature in fish pathogen *Vibrio anguillarum*. *J. Microbiol.* 55, 44–55. doi: 10.1007/s12275-017-6370-2

Miyamoto, Y., Koh, Y. H., Park, Y. S., Fujiwara, N., Sakiyama, H., Misonou, Y., et al. (2003). Oxidative stress caused by inactivation of glutathione peroxidase and adaptive responses. *Biol. Chem.* 384, 567–574. doi: 10.1515/BC.2003.064

Ng, W. O., Grossman, A. R., and Bhaya, D. (2003). Multiple light inputs control phototaxis in *Synechocystis* sp. strain PCC6803. *J. Bacteriol.* 185, 1599–1607. doi: 10.1128/JB.185.5.1599-1607.2003

Nishibuchi, M., and Kaper, J. B. (1995). Thermostable direct hemolysin gene of *Vibrio parahaemolyticus*: A virulence gene acquired by a marine bacterium. *Infect. Immun.* 63, 2093–2099. doi: 10.1128/iai.63.6.2093-2099.1995

O'Brien, M., and Colwell, R. (1985). Modified taurocholate-tellurite-gelatin agar for improved differentiation of *Vibrio* species. *J. Clin. Microbiol.* 22, 1011–1013. doi: 10.1128/jcm.22.6.1011-1013.1985

Okada, R., Matsuda, S., and Iida, T. (2017). *Vibrio parahaemolyticus* VtrA is a membrane-bound regulator and is activated *via* oligomerization. *PloS One* 12, e0187846. doi: 10.1371/journal.pone.0187846

Oladepo, S. A., and Loppnow, G. R. (2010). The effect of tryptophan on UV-induced DNA photodamage. *Photochem. Photobiol.* 86, 844–851. doi: 10.1111/j.1751-1097.2010.00745.x

Ongagna-Yhombi, S. Y., and Boyd, E. F. (2013). Biosynthesis of the osmoprotectant ectoine, but not glycine betaine, is critical for survival of osmotically stressed *Vibrio parahaemolyticus* cells. *Appl. Environ. Microbiol.* 79, 5038–5049. doi: 10.1128/AEM.01008-13

Ono, T., Park, K.-S., Ueta, M., Iida, T., and Honda, T. (2006). Identification of proteins secreted *via vibrio parahaemolyticus* type III secretion system 1. *Infect. Immun.* 74, 1032–1042. doi: 10.1128/IAI.74.2.1032-1042.2006

Overbeek, R., Olson, R., Pusch, G. D., Olsen, G. J., Davis, J. J., Disz, T., et al. (2014). The SEED and the rapid annotation of microbial genomes using subsystems technology (RAST). *Nucleic Acids Res.* 42, D206–D214. doi: 10.1093/nar/gkt1226

Ozasa, K., Won, J., Song, S., Tamaki, S., Ishikawa, T., and Maeda, M. (2017). Temporal change of photophobic step-up responses of *Euglena gracilis* investigated through motion analysis. *PloS One* 12, e0172813. doi: 10.1371/journal.pone.0172813

Park, K.-S., Ono, T., Rokuda, M., Jang, M.-H., Iida, T., Honda, T., et al. (2004a). Cytotoxicity and enterotoxicity of the thermostable direct hemolysin-deletion mutants of *Vibrio parahaemolyticus*. microbiol. *Immunol.* 48, 313–318. doi: 10.1111/j.1348-0421.2004.tb03512.x

Park, K.-S., Ono, T., Rokuda, M., Jang, M.-H., Okada, K., and Iida, T. (2004b). Functional characterization of two type III secretion systems of *Vibrio parahaemolyticus*. infect. *Immun.* 72, 6659–6665. doi: 10.1128/IAI.72.11.6659-6665.2004

Pattison, P. M., Tsao, J. Y., Brainard, G. C., and Bugbee, B. (2018). LEDs For photons, physiology and food. *Nature* 563, 493–500. doi: 10.1038/s41586-018-0706-x

Pazhani, G. P., Chowdhury, G., and Ramamurthy, T. (2021). Adaptations of *Vibrio parahaemolyticus* to stress during environmental survival, host colonization, and infection. *Front. Microbiol.* 12. doi: 10.3389/fmicb.2021.737299

Pflughoeft, K. J., Kierek, K., and Watnick, P. I. (2003). Role of ectoine in *Vibrio cholerae* osmoadaptation. *Appl. Environ. Microbiol.* 69, 5919–5927. doi: 10.1128/AEM.69.10.5919-5927.2003

Py, B., and Barras, F. (2010). Building fe–s proteins: bacterial strategies. *Nat. Rev. Microbiol.* 8, 436–446. doi: 10.1038/nrmicro2356

Raguénès, G., Christen, R., Guezennec, J., Pignet, P., and Barbier, G. (1997). *Vibrio diabolicus* sp. nov., a new polysaccharide-secreting organism isolated from a deep-sea hydrothermal vent polychaete annelid, *Alvinella pompejana*. *Int. J. Syst. Bacteriol.* 47, 989–995. doi: 10.1099/00207713-47-4-989

Remes, B., Eisenhardt, B. D., Srinivasan, V., and Klug, G. (2015). IscR of *Rhodobacter sphaeroides* functions as repressor of genes for iron-sulfur metabolism and represents a new type of iron-sulfur-binding protein. *Microbiologyopen* 4, 790–802. doi: 10.1002/mbo3.279

Reynolds, I. J., and Hastings, T. G. (1995). Glutamate induces the production of reactive oxygen species in cultured forebrain neurons following NMDA receptor activation. *J. Neurosci.* 15, 3318–3327. doi: 10.1523/JNEUROSCI.15-05-03318.1995

Sakazaki, R., Tamura, K., Kato, T., Obara, Y., Yamai, S., and Hobo, K. (1968). Studies on the enteropathogenic, facultatively halophilic bacteria, *Vibrio parahaemolyticus*. *Japanese J. Med. Sci. Biol.* 21, 325–331. doi: 10.7883/yoken1952.21.325

Sánchez de Miguel, A., Bennie, J., Rosenfeld, E., Dzurjak, S., and Gaston, K. J. (2022). Environmental risks from artificial nighttime lighting widespread and increasing across Europe. *Sci. Adv.* 8, eabl6891. doi: 10.1126/sciadv.abl6891

Shabala, L., and Ross, T. (2008). Cyclopropane fatty acids improve *Escherichia coli* survival in acidified minimal media by reducing membrane permeability to h^+ and enhanced ability to extrude h+. *Res. Microbiol.* 159, 458–461. doi: 10.1016/j.resmic.2008.04.011

Shinoda, S. (2011). Sixty years from the discovery of *Vibrio parahaemolyticus* and some recollections. *Biocontrol Sci.* 16, 129–137. doi: 10.4265/bio.16.129

Sugiyama, T., Iida, T., Izutsu, K., Park, K.-S., and Honda, T. (2008). Precise region and the character of the pathogenicity island in clinical *Vibrio parahaemolyticus* strains. *J. Bacteriol.* 190, 1835–1837. doi: 10.1128/JB.01293-07

Su, Z., Lian, G., Mawatari, K., Tang, P., He, S., Shimohata, T., et al. (2015). Identification and purification of the CPD photolyase in *Vibrio parahaemolyticus* RIMD2210633. *Photochem. Photobiol.* 91, 1165–1172. doi: 10.1111/php.12481

Takano, H., Beppu, T., and Ueda, K. (2006). The CarA/LitR-family transcriptional regulator: Its possible role as a photosensor and wide distribution in non-phototrophic bacteria. *Biosci. Biotechnol. Biochem.* 70, 2320–2324. doi: 10.1271/bbb.60230

Tardu, M., Bulut, S., and Kavakli, I. H. (2017). MerR and ChrR mediate blue light induced photo-oxidative stress response at the transcriptional level in *Vibrio cholerae*. *Sci. Rep.* 7, 40817. doi: 10.1038/srep40817

Tschowri, N., Busse, S., and Hengge, R. (2009). The BLUF-EAL protein YcgF acts as a direct anti-repressor in a blue-light response of *Escherichia coli*. *Genes Dev.* 23, 522–534. doi: 10.1101/gad.499409

Urmersbach, S., Alter, T., Koralage, M. S. G., Sperling, L., Gerdts, G., Messelhäusser, U., et al. (2014). Population analysis of *Vibrio parahaemolyticus* originating from different geographical regions demonstrates a high genetic diversity. *BMC Microbiol.* 14, 59. doi: 10.1186/1471-2180-14-59

Yoshida, A., Sasaki, H., Toyama, T., Araki, M., Fujioka, J., Tsukiyama, K., et al. (2017). Antimicrobial effect of blue light using *Porphyromonas gingivalis* pigment. *Sci. Rep.* 7, 5225. doi: 10.1038/s41598-017-05706-1

Zhang, Q., Dong, X., Chen, B., Zhang, Y., Zu, Y., and Li, W. (2016). Zebrafish as a useful model for zoonotic *Vibrio parahaemolyticus* pathogenicity in fish and human. *Dev. Comp. Immunol.* 55, 159–168. doi: 10.1016/j.dci.2015.10.021

Zhang, Y. M., and Rock, C. O. (2008). Membrane lipid homeostasis in bacteria. *Nat. Rev. Microbiol.* 6, 222–233. doi: 10.1038/nrmicro1839